

303660

**THE GLOBAL DISTRIBUTION OF OZONE DESTRUCTION RATES
OBTAINED FROM 13 YEARS OF NIMBUS/TOMS DATA (1979 - 1991)**

JAY R. HERMAN, R.S. STOLARSKI, R. MCPETERS

Code 916, NASA/Goddard Space Flight Center
Greenbelt, MD 20771

D. LARKO

Hughes-STX Corporation, 4400 Forbes Road
Lanham, MD 20706

ABSTRACT

Long-term ozone trends (percentage change) have been computed from 13 years of Nimbus/TOMS (Total Ozone Mapping Spectrometer) data as a function of latitude, longitude, and month for the period January 1, 1979 to December 31, 1991. In both hemispheres, the ozone column content has decreased at latitudes above 30° by amounts that are larger than predicted by homogeneous chemistry models for the 13-year time period. The largest rates of ozone decrease occur in the southern hemisphere during winter and spring, with recovery during the summer and autumn. The large winter ozone loss rates are consistent with observed low stratospheric temperatures, ice-cloud formation, and heterogeneous chemistry at middle and high latitudes. There are similar, but smaller changes observed in the northern hemisphere. At midlatitudes (40°N to 50°N) there are increased zonal average ozone depletion rates that correspond to 5 geographically localized regions of increased ozone depletion rates. Only the equatorial band between ±20° shows little or no long-term ozone change since January, 1979. The long-term winter ozone depletion rate data for both hemispheres suggests that heterogeneous chemistry processes may operate over a wide range of latitudes during half of the year.

INTRODUCTION

Measured decreases in the global amount of ozone have exceeded the predicted amount based on a homogeneous chemistry model and the known injection rates of chlorine bearing compounds (mainly chlorofluorocarbons) into the atmosphere. The discovery (Farman, et al., 1985) and evolution of the springtime Antarctic ozone hole represents the clearest evidence of accelerated destruction of ozone by heterogeneous chemistry involving chlorine. More recent evidence indicates that accelerated destruction of ozone occurs outside of the Antarctic regions (WMO, 1990; Stolarski, et al., 1991). This study extends the work to include details of the latitudinal variation of ozone trends (12-year percentage change in ozone amount) for each month of the year. The results provide evidence of heterogeneous chemistry processes operating during the winter and spring months over an extended latitude range.

The ozone data from Nimbus/TOMS (Total Ozone Mapping Spectrometer) have been analyzed for global

average trends (Herman et al., 1991b) showing a decrease of $3.2 \pm 1.6\%$ per decade. Removal of solar cycle effects reduced the global average rate of ozone decrease to $2.6 \pm 1.6\%$ per decade. The global average results agree with a statistical study of latitudinal and global changes by Stolarski et al. (1991). Zonal averages of the 12-year ozone trends for each month have shown that regions of accelerated ozone destruction can extend to midlatitudes during the winter and spring months. We show that the zonally averaged ozone depletion rate has a local maximum (7% to 10% per decade) in the 40°N to 50°N latitude range from January to March. In the southern hemisphere, we show that the large midlatitude and polar ozone depletion rates occur before the appearance of the Antarctic ozone hole, and therefore are not the result of backfilling into the polar region.

The TOMS ozone data set has been obtained from a six channel (312.5, 317.5, 331.2, 339.8, 360, and 380nm) Fastie-Ebert downward-viewing spectrometer on board the Nimbus-7 polar orbiting sun-synchronous satellite (see Herman et al. 1991a and b).

The TOMS ozone data are examined for long-term trends for the period from January 1, 1979 to December 31, 1991. The daily ozone data are grouped into 2° x 5° latitude-longitude bins and averaged for each month. The latitude coverage for each month is set to eliminate regions where there is no sunlight for part of the month. Some of the ozone data obtained near the day-night terminator has reduced accuracy when the solar zenith angle is greater than 82° (mostly during the winter months). For larger solar zenith angles, the underlying radiance data may be usable, but the inversion to obtain ozone is uncertain. Contributors to the uncertainty include; 1. non-Lambertian surface reflectivities, 2. cloud and aerosol effects, and 3. spherical geometry corrections for multiple scattering at zenith angles above 85°.

LATITUDINAL ZONAL AVERAGE OZONE TRENDS

The ozone trend within each 2° latitude band is obtained from a linear least squares fit to the zonally averaged ozone data after removing the seasonal variation (Herman et al., 1991b). The seasonal variation is removed by the following procedure. First, average the daily ozone values from each year to form an average annual ozone

variation for each latitude band. Second, subtract the average annual ozone variation for each day from the corresponding ozone data within each latitude band. The net ozone trend in percent per decade (PD) is given in Figure 1.

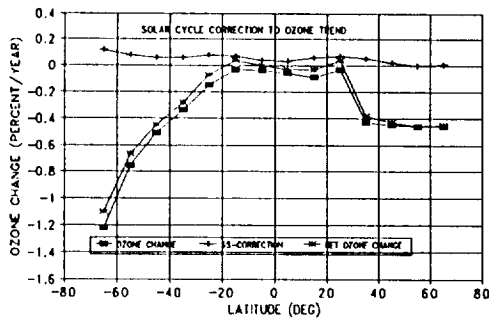


Figure 1. The zonally averaged ozone trend (percent loss per decade) as a function of latitude for the entire year. Also shown is an estimate of the solar cycle correction to the ozone trend of about +0.5% PD.

Each ozone time-series includes an apparent trend arising from solar cycle effects. For the 11.6-year time series considered in Herman et al. (1991b), the beginning time of the ozone data (November 1978) and the ending time (May 1990) are not symmetric with respect to the 10.7 cm solar radio flux ($F_{10.7}$) used as a surrogate for the solar ultraviolet variation (Bojkov et al., 1990). This effect can be removed from the ozone data by forming the fractional variation of $F_{10.7}$ and subtracting the results from the deseasonalized ozone data after the linear least squares trend has been removed (see equations 2, 3, and 4 of Herman et al., 1991). The solar correction at most latitudes is about 0.5% PD. This compares with the value computed for the global average data of 0.54% PD (see Figure 5 in Herman et al., 1991b). The apparent increase in the solar cycle correction near 65°S (1.2% PD) and the decrease near 65°N (0.1% PD) may not be significant because of the large seasonal and interannual variance at these latitudes. These results are in agreement with the statistical analysis of Stolarski et al. (1991). Similar asymmetry corrections have been computed for the 11- and 13-year ozone time series data. The results are 0.7% PD, 0.54% PD, 0.33, and 0.06% PD for 11-, 11.6-, 12-, and 13-year ozone time series, respectively.

The deseasonalized global average and zonal average ozone time series data show clear signs of wave structure of the same period as the 40 mb Singapore wind QBO (Quasi-biennial Oscillation) effect (see Herman et al., 1991b). The 40 mb Singapore winds show a 2% PD linear trend over the approximately 5 cycles between 1979 and 1991. Ozone time series can be reconstructed from the QBO and solar cycle terms and compared with the original deseasonalized ozone data (see Herman et al., 1991b).

Residual time series are obtained by subtracting the reconstructed time series from the original deseasonalized ozone time series for each latitude band. The results show that the small percentage change in the QBO signal does not contribute to a long-term ozone trend. However, there is a $\pm 1\%$ asymmetry effect with respect to the starting and ending points of the ozone time series relative to the phase of the QBO cycle at latitudes below 50°.

The trend analysis can be extended using more recent TOMS data (up to December 31, 1991). The extended period from May 1990 to December 1991 contains two periods of anomalous data. The first of these is related to an instrumental problem with the TOMS chopper wheel synchronization (see Herman et al., 1991a). The percentage of time that the chopper wheel was slightly out of synchronization increased to 70% (from the usual 1%) during the summer of 1990. The percentage returned to low values by October 1990 (less than 10%), and gradually returned to less than 1% for all of 1991. The effect on the ozone trend data was to slightly increase the noise content of the data and, therefore, the uncertainty of the trend determination. Since the period of time for the chopper wheel being out of synchronization was short (2 to 3 months), the effect of increased noise on the 12-year least squares fit to the deseasonalized data is much smaller than the total uncertainty of $\pm 1.4\%$ for the 1979 to 1990 period.

The second period of anomalous data is related to the Pinatubo volcanic eruption in June 1991. This eruption injected large amounts of SO_2 and dust into the stratosphere. The SO_2 is converted rapidly into small sulfuric acid aerosol particles that can remain resident in the stratosphere for many months. Adding this data to the ozone time series and computing long-term trends showed an apparent decrease in equatorial ozone between $\pm 15^\circ$ latitude. The equatorial ozone data measured by TOMS from June 1991 to November 1991 shows an aerosol scalloping effect centered on the 14 daily TOMS north-south orbital tracks. Based on radiative transfer calculations using the aerosol phase function (Torres et al., 1992), the zonal average values using all of the TOMS scan positions across an orbital track are very close to the correct values of zonal average ozone. Because of this, the effect of the Mt. Pinatubo aerosols on zonal average ozone trend determination is very small. Instead, most of the apparent decrease in equatorial ozone arises from the QBO driven wave structure in the ozone time-series data, and does not represent a long term ozone depletion effect.

MONTHLY LATITUDINAL VARIATION IN OZONE TRENDS

To investigate localized geographical patterns in the long-term behavior of ozone by month, the daily ozone data averaged for each week were grouped into $2^\circ \times 5^\circ$ (latitude \times longitude) cells over the latitude range $\pm 85^\circ$. For each grid cell, the average weekly variation was subtracted from the ozone data on a week-by-week basis

(deseasonalized), and then averaged to form a monthly data set. "Months" consist of 4 or 5 whole weeks. The yearly pattern is 5 4 4 4 5 4 5 4 4 5 4 4 weeks per month, with the largest shift from the non-leap-year calendar being 4 days in January and February (shift = 4 4 1 -1 3 -1 3 0 -2 2 0 3 days/month). Next, the 12-year ozone trend was determined by using a linear least squares fit to the "deseasonalized" ozone data. Solar cycle effects could be removed by subtracting 0.33% PD from each ozone-trend cell. The QBO correction for the 12-year ozone time series is negligible.

The 12-years of ozone trend data were subdivided into monthly and seasonal groupings. The seasonal groupings are: 1. December, January, February, 2. March, April, May, 3. June, July, August, and 4. September, October, November, corresponding roughly to Northern hemisphere winter, spring, summer, and autumn. Data obtained during the summer months in both hemispheres can be analyzed for trends over the largest latitude range for which Nimbus/TOMS acquires data (0° to 90°). During the winter months, the range is restricted to approximately 0° to 65° . Linear least squares fits to the data within each 2° x 5° grid cell are made to determine the ozone trends from January 1, 1979 to December 31, 1990. Figure 2 contains the zonal average trends for each month as a function of latitude, and are grouped by season.

THE SOUTHERN HEMISPHERE OZONE DEPLETION

In the southern hemisphere, the computed 12-year ozone depletion rates increase steadily from the equator towards the Antarctic. The larger depletion rates are in the winter, spring, and early summer (June through December), with the largest depletion rates occurring in the spring in conjunction with the ozone hole formation over the Antarctic region. Ozone depletion rates are observed to be in excess of 7% per decade over populated regions in South America poleward of -45° S (southern Argentina and the tip of New Zealand) for 7 months of the year. At the southernmost portion of South America the zonally averaged depletion rate is about 15% per decade during October.

Between -60° S and the equator, the ozone depletion rates (-6% to 0% per decade) are almost independent of the season during most of the summer and autumn months. During the winter, there are large increases in depletion rates between -80° S and -30° S, prior to the formation of the ozone hole. These large long-term depletion-rate increase during the winter months, -13% at 65° S, compared to summer and autumn, -5% to -8% from January to April, indicates that rapid chemical ozone destroying processes (possibly heterogeneous chemistry) are operating during the winter and spring, but at a slower rate than those within the ozone hole region. The large fall and winter depletion rates are not a carryover from previous year's springtime ozone hole, since there is a summer recovery to -5% depletion rates in January and February.

Even though the high latitude 12-year ozone depletion rate is large from June to December, rapid decreases in Antarctic ozone are not observed by TOMS until September, so that the large winter depletion rates (June, July, and August) are not the result of backfilling of an ozone hole. However, the persistence of large rates of ozone decrease into the midlatitude springtime may be enhanced by mixing with the ozone poor air from the Antarctic region.

Low atmospheric temperatures, the availability of particulates, and the sunrise conditions after the long polar night can account for differences in the rate of ozone destruction between the regions inside and outside of the south polar vortex. For example, the appearance of lower temperatures and the formation of stratospheric clouds and polar stratospheric clouds (PSCs) is greatly increased over Antarctica (PSC's, McCormick et al., 1982) compared to midlatitude regions during the winter months. As spring starts in the Antarctic region, temperatures rise, and the amount of active chlorine compounds increases rapidly in the lower stratosphere while the amount of active nitrogen compounds remains low. Aircraft flights into this region show the sudden rise of ClO (Brune et al., 1988, 1990) and OCIO (Wahner et al., 1989) and depletion of NO_2 at the region's boundary (Lowenstein et al., 1989). The elevated amounts of active chlorine and reduced nitrogen oxides lead to the rapid destruction of ozone observed for two months each Antarctic spring. The TOMS instruments on both the Nimbus and Meteor satellites see the rapid formation of the ozone hole each year within the south polar vortex region. Observations of the daily variation of ozone amount from TOMS do not show any large regions in the southern hemisphere outside of the south polar vortex where there is a rapid ozone depletion beyond the normal seasonal cycle. However, the trends computed from the ozone data show definite enhanced long-term depletion rates during the winter and spring months.

NORTHERN HEMISPHERE OZONE DEPLETION

The long-term ozone depletion rates observed during the northern hemisphere winter and spring months appear to be similar to the larger long-term depletion rates in the southern hemisphere outside of ozone hole region. The similarity is primarily in the rapid change of ozone depletion rates as a function of season (see Figure 2). There are differences between some of the corresponding months (e.g., during December and June), and there is the absence of a north polar ozone hole during the spring. Two additional differences between the hemispheres are immediately apparent in Figure 2. First, the northern hemisphere long-term ozone depletion rate is smaller than the rate in the southern hemisphere, particularly during the winter and spring (6% to 8% at 55° N compared to 8% to 10% at -55° S). It is likely that the seasonal ozone depletion rate differences between the hemispheres are related to the different behavior of the winter-spring polar vortex winds

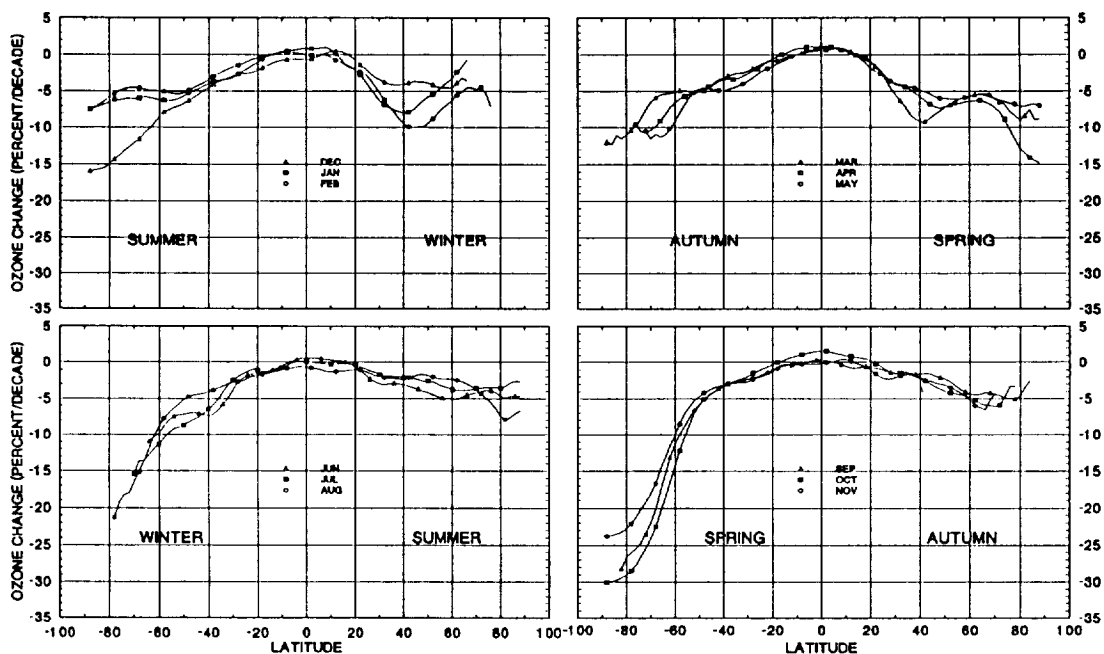


Figure 2. The zonal averages for long-term ozone percentage changes, from January 1, 1979 to December 31, 1990, computed for each month as a function of latitude. The ozone trend data were obtained from the daily TOMS measurements on a $2^{\circ} \times 5^{\circ}$ latitude by longitude grid, and then zonally averaged. The trend data was truncated as a function of latitude for those months where a portion of the period had days where there was no sunlight (e.g., polar winter).

and to the lower temperatures in the southern hemisphere winter causing the formation of more stratospheric ice particles.

Second, the winter-spring depletion rate maxima at 40°N to 50°N only appears as a small feature during the southern hemisphere winter. The local maxima do not appear in the estimates of northern hemisphere trends derived from the ground based Dobson spectrometer network (Bojkov, 1990) even though the general trends are consistent. These mid-latitude local maxima correspond to five regions of enhanced ozone depletion that appear in the northern hemisphere during the winter and spring months. The larger regions are located: 1. on the north-east coast of the United States, 2. on the north-west coast of the United States, 3. in the mid-Pacific ocean, and 4. over the northern portion of Russia. There is a geographically smaller region of enhanced depletion over the Scandinavian countries. It is unlikely that these local depletion regions signify any new depletion mechanisms, but rather are likely to be the result of long-term annually repeating transport of ozone-poor polar air to midlatitudes.

Northern hemisphere high latitude long-term ozone depletion rates, and the seasonal variation of these rates, are far larger than predicted using homogeneous chemistry models (Granier and Brasseur, 1992). Recent aircraft flights

into the Arctic have seen regions of enhanced ClO (Brune et al., 1988, 1990) and depleted NO_x (Kawa et al., 1990, and Wahner et al., 1990) in the lowest portions of the stratosphere. Satellite temperature measurements over the arctic (Newman et al., 1990) imply that PSC's can cover the region for periods on the order of weeks, and so provide the particulates for heterogeneous chemistry. Since Figure 2 shows that the long-term ozone depletion rate is smaller in the summer and autumn than in the winter and spring, the seasonal ozone destruction rate appears to be correlated with the onset of low temperatures and the appearance of stratospheric clouds. The long-term ozone depletion rate data are consistent with a reduced heterogeneous chemistry destruction rate for ozone (relative to the southern hemisphere) involving stratospheric particulates.

CONCLUSION

Long-term ozone trends (percent change) have been computed for 13 years of Nimbus/TOMS data as a function of latitude, longitude, and month for the period January 1, 1979 to December 31, 1991. Examination of the seasonal ozone trends for both the northern and southern polar regions reveal similarities and some differences in behavior. The most obvious difference between the two hemispheres is the much larger southern hemisphere decrease during the spring and winter. The large ozone

trend differences between the hemispheres probably arise from the different behavior of the north- and south-polar vortex winds, and the higher Arctic region winter temperatures. The result is that the Arctic depletion region is more irregular and smaller in magnitude than that in the Antarctic. The second major difference is the appearance of increased midlatitude ozone depletion rates in the vicinity of 30° to 50° during the winter and spring. These correspond to 5 localized depletion regions located: 1. on the north-east coast of the United States, 2. on the north-west coast of the United States, 3. in the mid-Pacific ocean, 4. over the northern portion of Russia, and 5. a smaller region of enhanced depletion over the Scandinavian countries. Since most of these are far south of the region where persistent stratospheric ice clouds, extremely low temperatures, and heterogeneous chemical reactions can produce long-term enhanced ozone depletion rates, they are likely to be the result of annually repetitive weather patterns involving the transport of high latitude air to midlatitudes. Until June, 1991, only the narrow region around the equator, between $\pm 20^\circ$, had no significant long-term ozone change compared to the amount of ozone present in 1978, when the Nimbus-TOMS instrument began measurements. After June 1991, the ozone time series for the equatorial region appears to show a significant decrease that might be associated with the Mt Pinatubo injection of SO₂ into the stratosphere. However, zonal average ozone amounts are almost unaffected by the presence of aerosols.

REFERENCES

- Bojkov, R., L. Bishop, W.J. Hill, C. Reinsel, and G.C. Tiao, A statistical analysis of revised Dobson total ozone data over the northern hemisphere, *J. Geophys. Res.*, **95**, 9785-9808, 1990.
- Bruno W.H., D.W. Toohey, J.G. Anderson, W.L. Starr, J.F. Vedder, and E.F. Danielsen, In situ northern midlatitude observations of ClO, O₃, and BrO, in the wintertime lower stratosphere, *Science*, **242**, 558, 1988.
- Bruno W.H., D.W. Toohey, J.G. Anderson, and K.R. Chan, In situ observations of ClO in the Arctic stratosphere: ER-2 aircraft results from 59°N to 80°N latitude, *Geophys. Res. Lett.* **17**, 505, 1990.
- Farman, J.C., B.D. Gardiner, and J.D. Shanklin, Large Losses of Ozone in Antarctica Reveal Seasonal ClO_x/NO_x Interaction, *Nature*, **315**, 207-210, 1985.
- Granier, C. and G. Brasseur, Impact of heterogeneous chemistry on model predictions of ozone changes, *J. Geophys. Res.*, **97**, Accepted for publication, 1992.
- Herman, J.R., R. Hudson, R. McPeters, R. Stolarski, Z. Ahmad, X-Y Gu, S. Taylor, and C. Wellemeyer, A new self-calibration method applied to TOMS/SBUV backscattered ultraviolet data to determine long-term global ozone change, *J. Geophys. Res.*, **96**, 7531-7545, 1991a.
- Herman, J. R., R. McPeters, R. Stolarski, D. Larko, and R. Hudson, Global Average Ozone Change From November 1978 to May 1990, *J. Geophys. Res.*, **96**, 17279-17305, 1991b.
- Kawa, S.R., D.W. Fahey, and L.C. Anderson, Measurement of Total Reactive Nitrogen During the Airborne Arctic Stratospheric Expedition, *Geophys. Res. Letters*, **17**, 485-488, 1990.
- Lowenstein, M., J.R. Podolske, K.R. Chan, and S.E. Strahan, Nitrous Oxide as a Dynamical Tracer in the 1987 Airborne Antarctic Ozone Experiment, *J. Geophys. Res.*, **94**, 11589-11598, 1989.
- McCormick, M.P., H.M. Steele, P. Hamill, W.P. Chu, and T.J. Swisher, Polar Stratospheric Cloud Sightings by SAM II, *J. Atmos. Sci.*, **39**, 1387-1397, 1982.
- McCormick, M.P., R.E. Veiga, and W.P. Chu, Stratospheric Ozone Profile and Total Ozone Trends Derived From the SAGE I and SAGE II Data, *Geophys. Res. Letters*, **19**, 269-272, 1992.
- Newman, P.A., L.R. Lait, M.R. Schoeberl, and R.M. Nagatani, Stratospheric temperatures during the northern hemisphere winter, *Geophys. Res. Lett.* **17**, 329-332, 1990.
- Stolarski, R.S., P. Bloomfield, R.D. McPeters, and J.R. Herman, Total Ozone Trends Deduced From Nimbus 7 TOMS Data, *Geophys. Res. Letters*, **6**, 1015-1018, 1991.
- Stolarski, R.S., L. Bishop, R. Bojkov, M.L. Chanin, V. Fioletov, V. Kirechhoff, J. Zawodny, and C. Zerefos, Chapter 2. Ozone and Temperature Trends, in Scientific Assessment of Ozone Depletion: 1991, WMO Ozone Report No. 25, 1992.
- Torres, O. P.K. Bhartia, J.R. Herman, Quadrennial Ozone Symposium, This Volume, 1992.
- Wahner, A., R.O. Jakoubek, G.H. Mount, A.R. Ravishankara, and A.L. Schmeltekopf, Remote sensing observations of nighttime OCIO during the Airborne Antarctic Ozone Experiment, *J. Geophys. Res.*, **94**, 11405, 1989.
- WMO, Report of the International Ozone Trends Panel: 1988, World Meteorological Organization, Global Ozone Research and Monitoring Project-Report No. 18, Geneva, Switzerland, 1990.